Effect of stress and free-carrier concentration on photoluminescence in InN

D. Y. Song,[1] M. E. Holtz,[1] A. Chandolu,[1] A. Bernussi,[1] S. A. Nikishin,[1] M. W. Holtz,[1,a)] and I. Gherasoiu[2]
[1]*Nano Tech Center, Texas Tech University, Lubbock, Texas 79409, USA*
[2]*Veeco Instruments Inc., MBE Operations, 4900 Constellation Drive, St. Paul, Minnesota 55127, USA*

(Received 16 February 2008; accepted 27 February 2008; published online 26 March 2008)

We report photoluminescence (PL) studies of InN epilayers grown by plasma-assisted molecular beam epitaxy with free-electron concentration ranging from 5.9×10^{17} to 4.2×10^{18} cm^{-3}. X-ray diffraction measurements are used to determine strains, which are best described as a combination of hydrostatic and biaxial. The PL energy is affected by both strains along with free-carrier concentration through band filling. PL spectra are used to estimate the dependence of the Fermi level on free-carrier concentration, taking strain into account. The fundamental energy gap is found to be ~0.70 eV. PL broadening is well described based on band filling. © *2008 American Institute of Physics*. [DOI: 10.1063/1.2899941]

The energy gap of InN has been the subject of controversy due to the large range of reported values. These have ranged from ~0.7 (Refs. 1 and 2) to 2 eV.[3] Variations in the literature have been attributed to deviations in the In composition as a result of cluster formation.[4] An alternative explanation for the range of optical gaps of InN, which is gaining broad acceptance, interprets the observations based on free-carrier concentration and the consequent band filling.[2,5] In the latter interpretation, the fundamental energy gap of InN is found to be 0.7 eV. This interesting development potentially extends the group-III-nitride semiconductors to span from the deep ultraviolet into near infrared wavelength range.

InN is generally grown on foreign substrates such as sapphire and buffer layers or template substrates are commonly used to initiate epitaxy. The mismatches between lattice constants and thermal expansion coefficients of InN and substrates lead to residual strains which are generally considered biaxial. The presence of dense extended or point defects may result in internal strains which are described as hydrostatic.[6,7] Thus, in general, the strain state must be considered as combined hydrostatic[8] and biaxial.[9]

In this paper, we consider the effects of residual stress and free-electron concentration on the observed photoluminescence (PL) spectrum of InN with low free-carrier concentration, 5.9×10^{17}–4.2×10^{18} cm^{-3}, and implications for the associated optical and fundamental energy gaps. We find that the strains are best described as a superposition of biaxial and hydrostatic and that the PL spectrum is affected by both of these strains along with carrier concentration.

InN was grown using plasma-assisted molecular beam epitaxy. A 300 nm thick buffer layer of GaN was first grown at 720 °C on sapphire substrates. The wafer temperature was reduced to the growth temperature, from 460–590 °C, and ~1 μm thick InN layers were grown. InN was characterized using x-ray diffraction (XRD), PL, and free-carrier concentrations determined by room temperature (RT) Hall measurements. More details may be found in Ref. 10. As-grown InN exhibits unintentional *n*-type conductivity. Recent work attributes this to the combined effects of surface electron accumulation, background donor density from impurities, and the nitrogen vacancy associated with dislocations.[11]

XRD symmetric (0002) and asymmetric $(10\bar{1}5)$ reflection measurements were performed to evaluate the RT lattice constants a and c. Representative diffraction patterns of InN with electron concentration of 9.8×10^{17} cm^{-3} are shown in Fig. 1. Measured a and c lattice constants differ from the $a_0=3.538$ Å and $c_0=5.703$ Å of relaxed InN.[12] Strains are determined using $e_a=(a-a_0)/a_0$ and $e_c=(c-c_0)/c_0$. The in-plane strains are generally biaxial compressive and $e_a\sim10^{-3}$ in magnitude are primarily attributed to thermal strain induced by the sapphire substrate when cooling from growth temperature to ambient. Values of the Poisson ratio υ, obtained using XRD measurements and $e_c/e_a=2\upsilon/(1-\upsilon)$, vary between 0.06 and 0.18. This suggests that the strain states are not solely biaxial and are better described as a superposition of hydrostatic and biaxial strains.[13]

The stress tensor σ is related to the strain tensor e through $\sigma=Ce$, where C is the elastic stiffness tensor.[13,14] Assuming the strain tensor to be diagonal, it may be written

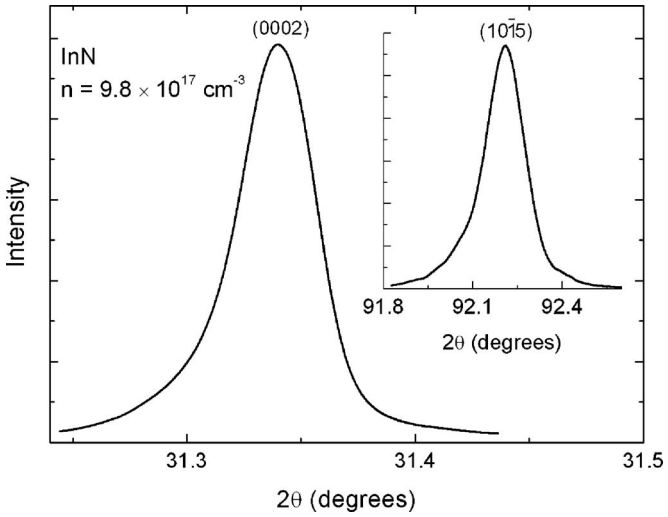

FIG. 1. Representative XRD symmetric (0002) and asymmetric $(10\bar{1}5)$ reflections for free-carrier concentration of 9.8×10^{17} cm^{-3}.

a)Author to whom correspondence should be addressed. Electronic mail: mark.holtz@ttu.edu.

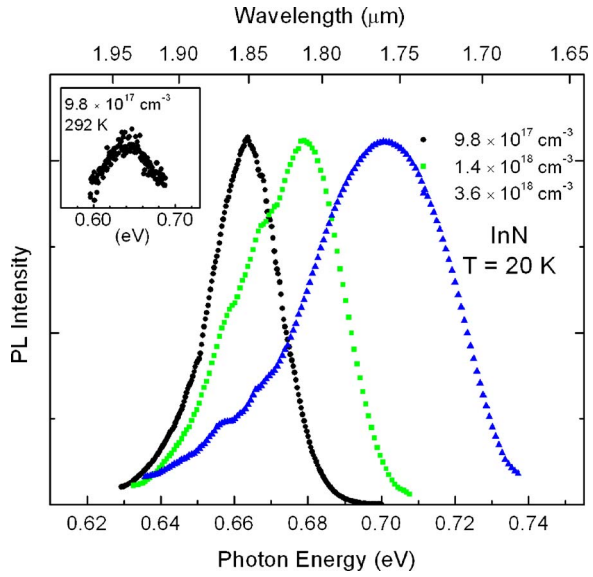

FIG. 2. (Color online) PL spectra (20 K) obtained for various free-carrier concentrations. The inset shows the corresponding RT measurement for free-carrier concentration of 9.8×10^{17} cm^{-3}.

$$e = \begin{bmatrix} e_a - \Delta e_a(T) & & \\ & e_a - \Delta e_a(T) & \\ & & e_c - \Delta e_c(T) \end{bmatrix}, \tag{1}$$

where[6]

$$\Delta e_{a(c)}(T) = \frac{\int_{RT}^{T}[\alpha_{a(c)}^{\text{sub}}(T') - \alpha_{a(c)}^{\text{film}}(T')]dT'}{1 + \int_{RT}^{T}\alpha_{a(c)}^{\text{film}}(T')dT'} \tag{2}$$

describes the induced thermal strain when deviating from reference RT to temperature T, and $\alpha_{a(c)}$ are temperature-dependent thermal expansion coefficients perpendicular and parallel to c axis, respectively. Strains are determined from RT XRD measurements. The associated stress is expressed as

$$\sigma = -P\begin{bmatrix} 1 & & \\ & 1 & \\ & & 1 \end{bmatrix} + \sigma_b\begin{bmatrix} 1 & & \\ & 1 & \\ & & 0 \end{bmatrix}, \tag{3}$$

where P is the hydrostatic pressure and σ_b is the biaxial stress. We use published data for the temperature dependent thermal expansion coefficients of InN (Ref. 15) and sapphire[16] and elastic stiffness constants of InN.[17] Measured values of e_a and e_c allow us to estimate both the hydrostatic pressure P and the biaxial stress σ_b of our InN at RT. Using Eqs. (1)–(3), we also obtain the stress at $T=20$ K relevant to our PL measurements. The values of Δe_a and Δe_c at $T=20$ K are 6×10^{-5} and 2×10^{-5}, respectively. These values are small, $\sim 1/20$ of the measured strains.

The PL spectra were obtained with the samples mounted in a closed-cycle cryostat, excited using light from a Kr-ion laser (647.1 nm) and detected using a cooled InAs photodetector. Figure 2 shows low temperature ($T=20$ K) PL spectra of InN films with several electron concentrations. Each spectrum exhibits a single strong emission near 0.7 eV attributed to the near band edge emission.[9] The PL spectra (Burstein–Moss) blueshift with increasing electron concentration as the Fermi level (E_F) moves into the conduction band (CB).[2] The inset of Fig. 1 shows the RT PL spectrum of InN with electron concentration of 9.8×10^{17} cm^{-3}. The band edge emission redshifts by $\sim$33 meV and broadens with increasing temperature, which is attributed to lattice expansion and electron-phonon interaction.[18,19]

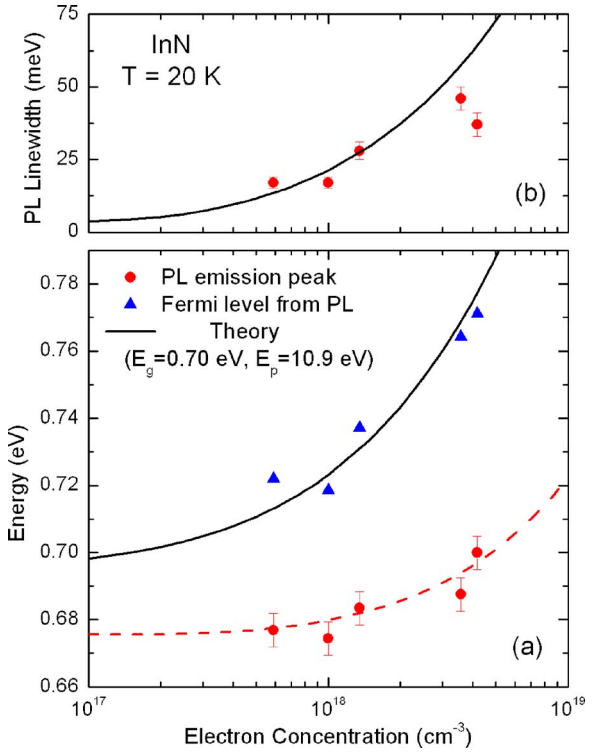

FIG. 3. (Color online) Low temperature (20 K) InN PL peak energy and Fermi level (a) and PL linewidth (b) as a function of the free-electron concentration. The solid curve in (a) is a theoretical fit. The dashed curve in (a) is a guide to the eye. The solid curve in (b) is calculated based on luminescence intensity function taking into account band filling effect.

Compressive biaxial stress decreases the band gap according to $\Delta E_b = k_b\sigma_b$, where $k_b=-55$ meV/GPa is the stress coefficient.[9] Hydrostatic pressure also influences the band structure of InN.[8] For our samples, with free-electron concentration of $\sim10^{18}$ cm^{-3}, we use $\Delta E_P = k_H P$ with $k_H = 25$ meV/GPa.[8] To remove the effects of stress and obtain the dependence of the band gap on the free-electron concentration, we use strains obtained from XRD measurements and Eqs. (1)–(3) to obtain P and σ_b. In our samples, the hydrostatic stresses vary from -0.04 to -0.29 GPa, where $P<0$ implies tensile, with corresponding band gap redshifts of 1–7 meV. Our values for σ_b range from -0.05 to -0.52 GPa, producing blueshifts from $\sim$3 to 29 meV for the band gap. PL peak positions, corrected for the strain-induced shifts, are plotted in Fig. 3(a) as a function of free-electron concentration.

Band filling and band gap renormalization contribute to the observed variation in PL peak position with changing free-electron concentration. In heavily doped n-type semiconductors, band filling may move E_F inside the CB. PL emission at low pump intensity may involve any of the occupied CB states, i.e., those below E_F, and the top of the valence band. Thus, as band filling causes E_F to shift higher into the CB, the PL peak blueshifts, as seen in Figs. 2 and 3(a) and broadens as in Figs. 2 and 3(b). Because the PL peak position is a convolution of density of states, occupation factor, and the matrix elements between the participating electron and hole states, it serves only as an estimate of the band gap and E_F. A better approach is to use the uppermost energy of the PL band, which should approximate E_F. Esti-

mates of the obtained E_F values are summarized in Fig. 3(a).

Wu *et al.* have examined the shift in the InN absorption edge with carrier concentration and have applied Kane's $\mathbf{k}\cdot\mathbf{p}$ model to describe the dependence.[2] Carrier concentration dependent effective masses are used to calculate E_F and the lowest CB of InN is found to be nonparabolic. Neglecting spin-orbit and crystal field splitting, along with higher order perturbations from remote bands, the CB dispersion is

$$E_C(k) = E_G + \frac{\hbar^2 k^2}{2m_0} + \frac{1}{2}\left(\sqrt{E_G^2 + 4E_p\frac{\hbar^2 k^2}{2m_0}} - E_G\right), \tag{4}$$

where E_G is the band gap and E_p is related to the momentum matrix element $E_p = 2/m_0|\langle S|p_x|X\rangle|^2$, where $|X\rangle$ and $|S\rangle$ are wave functions of the valence and CB states, respectively.[2]

CB renormalization describes interactions between electrons (electron-electron) and between electrons and ionized point impurities. The magnitude of the CB shift stemming from the electron-electron interactions is.[2]

$$\Delta E_{e-e} = \frac{2e^2 k_F}{\pi\varepsilon_s}\left[1 + \frac{\lambda_\pi}{2k_F} - \frac{\lambda}{k_F}\tan^{-1}\left(\frac{k_F}{k_{TF}}\right)\right], \tag{5}$$

where $k_F = (3\pi^2 n)^{1/3}$ is the Fermi wavevector, $k_{\mathrm{TF}} = (2/\sqrt{\pi}) \times (k_F/\alpha_B)^{1/2}$ is the Thomas–Fermi screening wavevector, ε_s is the static dielectric constant, and $\alpha_B = 0.53\varepsilon_S m_0/m_e^*$ is the Bohr radius in Å. The n-dependent electron effective mass m_e^* is taken from Ref. 2. The magnitude of the CB shift resulting from electron-ionized impurity interaction is

$$\Delta E_{e-i} = \frac{4\pi n e^2}{a_B \varepsilon_s k_{\mathrm{TF}}^3}. \tag{6}$$

Combining these interactions, E_F shifts according to $E_C(k_F) - \Delta E_{e-e} - \Delta E_{e-i}$.

Using E_g and E_p as fitting parameters, we obtain the solid curve in Fig. 3(a). Fit parameters $E_g \sim 0.70$ eV and $E_p \sim 10.9$ eV produce good agreement with the E_F results. The fit parameters agree with previously reported values of 0.7 and 10 eV based on absorption edges[2] and effective masses.[20] We note that applying the band filling and renormalization approach to the PL peak positions results in a slightly lower E_g, as expected, and a very low $E_p \sim 4$ eV. The small E_p value is due to the shallower free-carrier dependence seen in the PL peak energy when compared with the Fermi level. The shallow dependence arises because the spectrum is a weighted average of the states between the CB minimum and E_F and not a direct measure of either quantity for free-electron concentrations in this range and higher.

At high free-electron concentration band filling is important in determining the PL spectrum. The emission spectrum can be derived using Fermi's rule, taking into account density of states, occupation factors, and matrix elements. Assuming the latter is a slowly varying function, the intensity can be approximated by[21]

$$I(E) \propto (E - E_G)^{1/2}\left\{1 + \exp\left[\frac{m_h^*}{m_e^* + m_h^*}\frac{E - E_G}{k_B T} - \frac{E_C(k_F)}{k_B T}\right]\right\}^{-1}, \tag{7}$$

where m_h^* is the hole effective mass and k_B is the Boltzmann constant. In Eq. (7), m_e^* and k_F depend on carrier concentration. Comparison of calculated and measured linewidth as a function of free-electron concentration, shown in Fig. 3(b), produces good agreement. This suggests that band filling is the dominant mechanism responsible for the PL broadening observed in the InN investigated in this work.

In conclusion, the low temperature PL spectra of InN epilayers have been studied for low free-electron concentrations. Values of the Poisson ratio, obtained using XRD, vary between 0.06 and 0.18, indicating a superposition of hydrostatic and biaxial strains in the InN. Hydrostatic stresses range from −0.04 to −0.29 GPa, with corresponding band gap redshifts of 1–7 meV. The biaxial stresses range from −0.05 to −0.52 GPa, resulting in blueshifts from ~3 to 29 meV for the band gap. These shifts are comparable in magnitude to the shifts attributed to carrier concentrations in the range studied here and must be taken into account in order to determine the band gap of InN. Values for E_F are estimated from the uppermost energy of the PL. The free-electron concentration dependence of E_F, corrected for the strain-induced shifts, is well described by Kane's $\mathbf{k}\cdot\mathbf{p}$ model and CB renormalization. The PL linewidth broadening is well described by the band filling.

Work at Texas Tech University was supported by the National Science Foundation (ECS-0609416 and ECS-0304224), U.S. Army CERDEC Contract (W15P7T-07-D-P040), and the J. F Maddox Foundation.

[1] V. Y. Davydov, A. A. Klochikhin, R. P. Seisyan, V. V. Emtsev, S. V. Ivanov, F. Bechstedt, J. Furthmuller, H. Harima, V. Mudryi, J. Aderhold, O. Semchinova, and J. Graul, Phys. Status Solidi B **229**, R1 (2002).
[2] J. Wu, W. Walukiewicz, W. Shan, K. M. Yu, J. W. Ager, E. E. Haller, H. Lu, and W. J. Schaff, Phys. Rev. B **66**, 201403 (2002).
[3] Q. X. Guo and A. Yoshida, Jpn. J. Appl. Phys., Part 1 **33**, 2453 (1994).
[4] T. V. Shubina, S. V. Ivanov, V. N. Jmerik, D. D. Solnyshkov, V. A. Vekshin, P. S. Kop'ev, A. Vasson, J. Leymarie, A. Kavokin, H. Amano, K. Shimono, A. Kasic, and B. Monemar, Phys. Rev. Lett. **92**, 117407 (2004).
[5] D. Y. Song, V. Kuryatkov, M. Basavaraj, D. Rosenbladt, S. A. Nikishin, M. Holtz, A. L. Syrkin, A. S. Usikov, V. A. Ivantsov, and V. A. Dmitriev, J. Appl. Phys. **99**, 116103 (2006).
[6] I. Ahmad, M. Holtz, N. N. Faleev, and H. Temkin, J. Appl. Phys. **95**, 1692 (2004).
[7] C. Kisielowski, J. Kruger, S. Ruvimov, T. Suski, J. W. Ager, E. Jones, Z. Liliental Weber, M. Rubin, E. R. Weber, M. D. Bremser, and R. F. Davis, Phys. Rev. B **54**, 17745 (1996).
[8] A. Kaminska, G. Franssen, T. Suski, I. Gorczyca, N. E. Christensen, A. Svane, A. Suchocki, H. Lu, W. J. Schaff, E. Dimakis, and A. Georgakilas, Phys. Rev. B **76**, 075203 (2007).
[9] X. Q. Wang, S. B. Che, Y. Ishitani, and A. Yoshikawa, J. Appl. Phys. **99**, 073512 (2006).
[10] I. Gherasoiu, M. O'Steen, T. Bird, D. Gotthold, A. Chandolu, D. Y. Song, S. X. Xu, M. Holtz, S. A. Nikishin, and W. J. Schaff, J. Vac. Sci. Technol. A (to be published).
[11] L. F. J. Piper, T. D. Veal, C. F. McConville, H. Lu, and W. J. Schaff, Appl. Phys. Lett. **88**, 252109 (2006).
[12] X. Q. Wang, S. B. Che, Y. Ishitani, and A. Yoshikawa, Appl. Phys. Lett. **89**, 171907 (2006).
[13] G. Kipshidze, B. Yavich, A. Chandolu, J. Yun, V. Kuryatkov, I. Ahmad, D. Aurongzeb, M. Holtz, and H. Temkin, Appl. Phys. Lett. **86**, 033104 (2005).
[14] R. G. Lee, A. Idesman, L. Nyakiti, and J. Chaudhuri, J. Appl. Phys. **102**, 063525 (2007).
[15] K. Wang and R. R. Reeber, Appl. Phys. Lett. **79**, 1602 (2001).
[16] M. Leszczynski, T. Suski, H. Teisseyre, P. Perlin, I. Grzegory, J. Jun, S. Porowski, and T. D. Moustakas, J. Appl. Phys. **76**, 4909 (1994).
[17] A. F. Wright, J. Appl. Phys. **82**, 2833 (1997).
[18] C. L. Hsiao, H. C. Hsu, L. C. Chen, C. T. Wu, C. W. Chen, M. Chen, L. W. Tu, and K. H. Chen, Appl. Phys. Lett. **91**, 181912 (2007).
[19] D. Y. Song, M. Basavaraj, S. A. Nikishin, M. Holtz, V. Soukhoveev, A. Usikov, and V. Dmitriev, J. Appl. Phys. **100**, 113504 (2006).
[20] S. P. Fu and Y. F. Chen, Appl. Phys. Lett. **85**, 1523 (2004).
[21] D. S. Jiang, Y. Makita, K. Ploog, and H. J. Queisser, J. Appl. Phys. **53**, 999 (1982).